Bioorganic & Medicinal Chemistry 20 (2012) 2141–2151

Contents lists available at SciVerse ScienceDirect

Bioorganic & Medicinal Chemistry

journal homepage: www.elsevier.com/locate/bmc

Synthesis, biological evaluation and molecular investigation of fluorinated peroxisome proliferator-activated receptors α/γ dual agonists

Giuseppe Fracchiolla [a], Antonio Laghezza [a], Luca Piemontese [a], Mariagiovanna Parente [a], Antonio Lavecchia [b,*], Giorgio Pochetti [c], Roberta Montanari [c], Carmen Di Giovanni [b], Giuseppe Carbonara [a], Paolo Tortorella [a], Ettore Novellino [b], Fulvio Loiodice [a,*]

[a] Dipartimento Farmaco-Chimico, Università degli Studi di Bari 'Aldo Moro', Via Orabona 4, 70126 Bari, Italy
[b] Dipartimento di Chimica Farmaceutica e Tossicologica, 'Drug Discovery' Laboratory, Università di Napoli 'Federico II', Via Domenico Montesano 49, 80131 Napoli, Italy
[c] Istituto di Cristallografia, Consiglio Nazionale delle Ricerche, Montelibretti, 00016 Monterotondo Stazione, Roma, Italy

ARTICLE INFO

Article history:
Received 21 October 2011
Revised 13 January 2012
Accepted 16 January 2012
Available online 28 January 2012

Keywords:
Structure–activity relationships
Carboxylic acids
Nuclear receptors
Crystallographic studies
Docking experiments

ABSTRACT

PPARs are transcription factors that govern lipid and glucose homeostasis and play a central role in cardiovascular disease, obesity, and diabetes. Thus, there is significant interest in developing new agonists for these receptors. Given that the introduction of fluorine generally has a profound effect on the physical and/or biological properties of the target molecule, we synthesized a series of fluorinated analogs of the previously reported compound **2**, some of which turned out to be remarkable PPARα and PPARγ dual agonists. Docking experiments were also carried out to gain insight into the interactions of the most active derivatives with both receptors.

1. Introduction

Peroxisome proliferator-activated receptors (PPARs) are members of the nuclear receptor superfamily, and three subtypes (PPARα, PPARγ, and PPARδ) have been identified to date. They control the expression of genes involved in fatty acid metabolism and function as cellular lipid sensors that activate transcription in response to the binding of a cognate ligand, generally fatty acids and their eicosanoids metabolites.[1,2]

PPARα is highly expressed in the liver and skeletal muscle and is the molecular target for the fibrates (e.g., fenofibrate and gemfibrozil), a class of drugs that lower plasma triglycerides and increase HDL cholesterol levels in humans.[3,4] PPARγ is the most extensively studied among the PPAR subtypes and plays important roles in the functions of adipocytes, muscles, and macrophages with a direct impact on type 2 diabetes, dyslipidemia, atherosclerosis, and cardiovascular diseases.[5,6] This receptor is expressed most abundantly in adipose tissue and mediates the antidiabetic activity of the insulin-sensitizing drugs belonging to the thiazolidinedione (TZD) class such as rosiglitazone and pioglitazone.[7] PPARδ is more ubiquitously distributed and recent evidence suggests that this isoform may govern diverse physiological processes, including the regulation of lipid and lipoprotein metabolism,[8] insulin sensitivity,[9] cardiac function,[10] epidermal biology,[11] neuroprotection,[12] and gastrointestinal tract function and disease.[13] To date, however, no PPARδ agonist has been fully developed and the clinical potential of targeting this isotype remains to be clearly determined.

Given the importance of simultaneously controlling both glucose and lipid levels, dual-acting PPARα/γ agonists, are considered a very attractive option in the treatment of dyslipidemic type 2 diabetes.[14–19] One of the key challenges for the development of a dual agonist is identifying the optimal receptor subtype selectivity ratio. In particular, PPARγ full agonists, despite their proven benefits, possess a number of deleterious side effects such as weight gain, peripheral edema, increased risks of congestive heart failure and higher rate of bone fracture.[20,21] During the last decade, therefore, new drugs acting as partial agonists or modulators of PPARγ have been developed with the goal of retaining the beneficial effects while reducing the adverse effects. A number of these drugs has already demonstrated desirable pharmacological profiles in various rodent models with significantly reduced side effects relative to those generally observed with existing full agonists.[22–29]

We recently reported a series of (*S*)-α-aryloxy-β-phenylpropanoic acids **1** (Fig. 1) some of which were potent PPARα agonists as well as PPARγ agonists.

For the partial PPARγ agonist **2**, the lower potency and efficacy on PPARγ was associated with a lower adipogenic effect distinguishing it from conventional PPARγ agonists and suggesting it is

* Corresponding authors. Fax: +39 081678613 (A.L.); +39 0805442231 (F.L.).
E-mail addresses: lavecchi@unina.it (A. Lavecchia), floiodice@farmchim.uniba.it (F. Loiodice).

0968-0896/$ - see front matter © 2012 Elsevier Ltd. All rights reserved.
doi:10.1016/j.bmc.2012.01.025

R = CF_3, CH_3O, $COCH_3$, Ph, C_2H_5, CH_2OH, 2-Th, Cl

Figure 1. (*S*)-α-aryloxy-β-phenylpropanoic acids endowed with PPARα/γ dual activity.

a PPARγ modulator.[30] In particular, due to the reduced efficiency in the stimulation of adipocyte differentiation and the ensuing fat accretion and weight gain, **2** could represent a very promising candidate as the lead for the design of new dual PPARα/PPARγ drugs to be used in the therapy of human metabolic disorders such as type 2 diabetes, atherosclerosis, and obesity in patients with high cardiovascular risk.

Due to the peculiarity of compound **2**, we decided to better understand its mechanism of action at the molecular level and, for this reason, solved the crystal structure of its complex with PPARγ-LBD. In addition, with the aim to investigate the possibility to fine-tune the activity of this ligand, we synthesized a new series of its analogs in which fluorine atom or trifluoromethyl group were introduced on the aromatic rings in place of chlorine or as additional substituents. Fluoro or trifluoromethyl substituents generally have a profound effect on the physical and/or biological properties of the target molecule. Their introduction, in fact, beyond improving metabolic stability by blocking metabolically labile sites, can modulate physicochemical properties, such as lipophilicity or acidity, change molecular conformation, and increase binding affinity by exploiting specific interactions of fluorine with the target protein.[31,32]

Herein we report, therefore, the crystal structure of the complex PPARγ-LBD/**2** as well as the synthesis and biological activity of the analogs shown in Figure 2.

In a first set of compounds (**3–8**), the chlorine atom was removed and substituted by either fluorine or trifluoromethyl group in different positions of the aryloxy group; in the set of compounds **9–17**, the chlorine atom was maintained in the para position of the phenoxy moiety, except for **17**, while introducing the same substituents either on one of the aromatic rings or both of them. The preparation of the analog **10** was carried out because, as previously shown,[33] the introduction of an additional chlorine on the benzylic moiety of **2** increased the potency on both PPARα and PPARγ isotypes. Finally, we prepared the fluoro analogs **18** and **19** in which the benzylic methylene was removed and the phenyl was directly linked to the stereogenic carbon by analogy with the active metabolite **20** of the known PPARγ selective modulator metaglidasen which is currently in Phase II clinical development as an oral uricosuric agent for the treatment of hyperuricemia in patients with type 2 diabetes.[34]

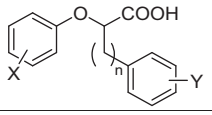

Cpd	Abs. Config.	X	Y	n
2	*S*	4-Cl	H	1
3	*S*	4-F	H	1
4	-	3-F	H	1
5	-	2-F	H	1
6	*S*	4-CF_3	H	1
7	*S*	3-CF_3	H	1
8	-	2-CF_3	H	1
9	*S*	4-Cl, 2-F	H	1
10	-	4-Cl, 2-F	4-Cl	1
***S*-10**	*S*	4-Cl, 2-F	4-Cl	1
11	-	4-Cl, 3-F	H	1
12	-	4-Cl, 3-CF_3	H	1
13	-	4-Cl	2-F	1
14	-	4-Cl	3-F	1
15	-	4-Cl	4-F	1
16	-	4-Cl, 2-F	3-F	1
17	-	2-CF_3	3-F	1
18	-	4-Cl, 2-F	H	0
19	-	4-Cl, 2-F	4-Cl	0
20	*(a)*	3-CF_3	4-Cl	0

Figure 2. Fluorinated α-aryloxy-β-phenylpropanoic acids reported in the present study. (a) The active metabolite (**20**) of metaglidasen is the levo-isomer of uncertain absolute configuration.

Considering the high degree of stereoselectivity generally displayed by PPARs towards S isomers, some derivatives were prepared, when synthetically feasible, only in this configuration (**3**, **6**, **7** and **9**); *S*-**10**, instead, was obtained by fractional crystallization of the diastereomeric esters achieved from racemate with (*R*)-pantolactone.

The PPARα and PPARγ activity of all derivatives was evaluated by the transactivation assay, a powerful and widely used assay that is generally accepted to correlate well with in vivo activity. For the most potent agonists **6** and *S*-**10** docking experiments were performed on both PPAR isoforms to gain more details on the interactions at a molecular level and propose a binding mode explaining the SAR data.

2. Results and discussion

2.1. Chemistry

Synthesis of compounds **3**–**5**, **7**–**9**, **11** and **12** was carried out as previously reported for analog **6**,[30] and is depicted in Scheme 1. The procedure started from ethyl phenyllactate and the suitable phenol, which were condensed, under slightly modified Mitsunobu conditions,[35] to give the corresponding ethyl ester intermediates. The saponification of these intermediates with 1 N NaOH solution in THF provided the desired final acids. For the S enantiomeric acids **3**, **6**, **7** and **9**, (*R*)-ethyl phenyllactate was used as starting compound.

Racemates **10** and **13**–**17** were prepared by condensation of the suitable diethyl ariloxymalonate, obtained as reported in a previous work,[36] with the appropriate substituted benzyl bromide in the presence of 95% NaH followed by alkaline hydrolysis and thermal decarboxylation at 160 °C (Scheme 2). The *S* isomer of compound **10** was obtained by fractional crystallization followed by alkaline hydrolysis of the diastereomeric esters mixture achieved through condensation of the racemate with *R*-pantolactone (Scheme 2).

The absolute configuration of this enantiomer was determined on the basis of circular dichroism analysis; the *S* configuration was assigned to the levorotatory isomer whose CD curve shows a negative Cotton effect in the 235–270 nm region and a positive Cotton effect around 225 nm. The same effects are also present in the CD curve of the isomer **9** which was used as a reference

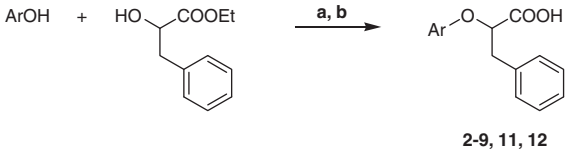

2-9, 11, 12

Scheme 1. Reagents and conditions: (a) DVB–Ph_3P, DIAD, anhydrous toluene, rt; (b) 1 N NaOH, THF, rt.

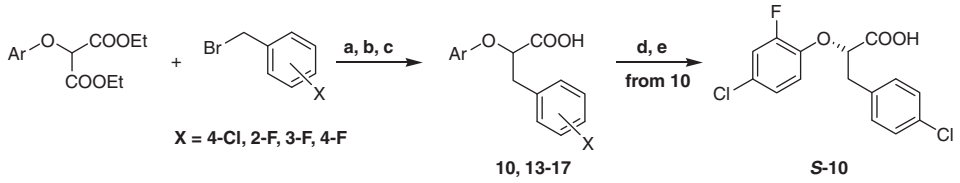

Scheme 2. Reagents and conditions: (a) 95% NaH powder, anhydrous DMF, 55 °C; (b) 1 N NaOH, 95% EtOH, reflux; (c) decarboxylation at 160 °C; (d) (*R*)-pantolactone, DCC, DMAP, anhydrous THF; fractional cristallization from *n*-hexane/$CHCl_3$; (e) 1 N NaOH, THF.

compound for its high structural similarity. The *S* configuration of **9**, in fact, was assigned on the basis of the known stereochemical course of its synthetic pathway.

Compounds **18** and **19** were obtained as described in Scheme 3 by condensation of sodium 4-chloro-2-fluorophenate with the corresponding ethyl 2-bromo-2-aryl acetate in absolute EtOH, followed by saponification of the ester intermediates.

All the optically active acids had enantiomeric excesses >98% as determined by HPLC analysis on chiral stationary phase (see Section 4).

2.2. Binding of 2 to PPARγ-LBD

Figure 1 of the Supplementary data shows the positioning of **2** fitted into the electron density map calculated in the hydrophobic pocket of PPARγ. The orientation of this ligand was similar to those previously reported for other α-aryloxy-β-phenylpropanoic acids.[35] Figure 3 summarizes the binding interactions made by the polar head of **2** with the residues that are generally involved in the canonical intermolecular H-bonding network in the presence of carboxylate containing ligands.

One of the carboxylate oxygens formed a bifurcated H-bond with the Y473 OH and the H323 Nε2 groups; the other carboxylate oxygen was at H-bonding distance from H449 Nε2 which, in turn, engaged the ligand ether oxygen in a further H-bond. Interestingly, also the chlorine atom, as previously reported for other substituents, was able to force the side chain of Phe282 to assume a new conformation allowing the access to the new region called 'diphenyl pocket'.[35] Moreover, the Cl atom made electrostatic interactions with the side-chain of Q286 and the sulphur atom of M463, contributing in this way to stabilize the conformation of the loop 11/12 (Fig. 4).

2.3. Pharmacology

Compounds **3**–**19** were evaluated for their agonist activity toward the human PPARα (hPPARα) and PPARγ (hPPARγ) subtypes in comparison with **2** and the active metabolite **20** of metaglidasen. For this purpose, GAL4-PPAR chimeric receptors were expressed in transiently transfected HepG2 cells according to a previously reported procedure.[30] The results obtained were also compared with corresponding data for Wy-14,643 and pioglitazone used as reference compounds in the PPARα and PPARγ transactivation assays,

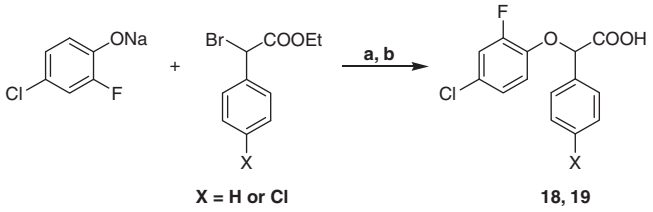

Scheme 3. Reagents and conditions: (a) abs EtOH, reflux; (b) 2 N NaOH, THF, rt.

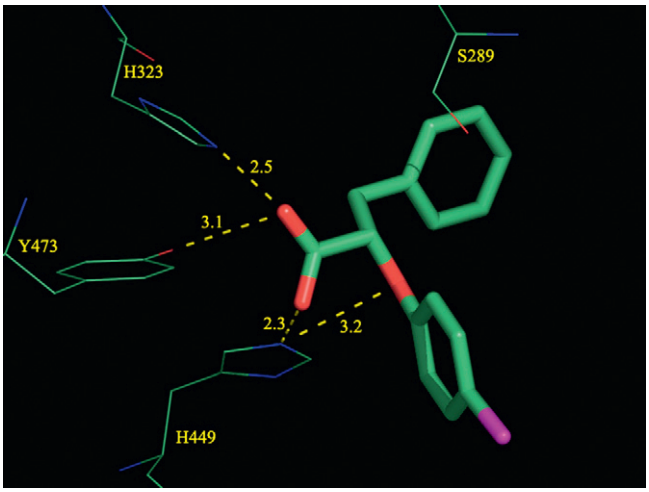

Figure 3. Hydrogen bond network of **2** in complex with PPARγ.

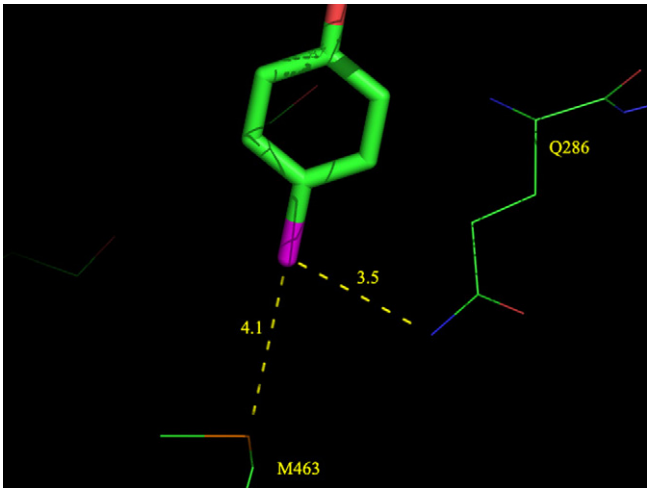

Figure 4. Chlorine atom interactions in the complex PPARγ/**2**.

respectively (Table 1). Maximum obtained fold induction with the reference agonist was defined as 100%.

The results obtained from compounds **3**–**8** showed that PPAR activity depends on the type and the position of the substituent. The para-fluoro derivative **3**, in fact, displayed a marked reduction of the activity on both PPAR isoforms compared to **2** and similar effects were obtained with the ortho-fluoro analogs **4** and **5** even though these compounds were tested as racemates.

On the contrary, trifluoromethyl analogs provided different results. In this case, in fact, the most potent derivative turned out to be the para-substituted analog **6**. This compound, in fact, showed sub-micromolar potency acting basically as a full agonist on PPARα and partial agonist on PPARγ. A remarkable decrease

Table 1
Activity of compounds tested in the cell-based transactivation assay

Compd	PPARα		PPARγ	
	EC_{50} (μM)	E_{max} (%)	EC_{50} (μM)	E_{max} (%)
2	4.9 ± 1.0	90 ± 3	9.6 ± 1.5	77 ± 8
3	24.8 ± 4.5	55 ± 3	35.2 ± 2.5	58 ± 9
4	21 ± 7	57 ± 6	41 ± 4	33 ± 3
5	22.3 ± 2.5	36 ± 6	19 ± 4	26 ± 2
6	0.5 ± 0.1	81 ± 11	0.9 ± 0.2	59 ± 9
7	9.8 ± 0.5	71 ± 4	15.9 ± 0.5	44 ± 11
8	i.a.	i.a.	30 ± 20	13 ± 6
9	2.2 ± 0.6	101 ± 5	2.5 ± 0.1	84 ± 10
10	1.4 ± 0.2	76 ± 12	0.9 ± 0.3	69 ± 6
S-**10**	1.0 ± 0.2	76 ± 22	0.5 ± 0.2	70 ± 9
11	6.5 ± 1.6	51 ± 6	14.1 ± 2.9	40 ± 9
12	2.5 ± 0.1	59 ± 11	5.8 ± 3.9	21 ± 11
13	6.6 ± 0.1	66 ± 2	4.9 ± 1.5	59 ± 4
14	5.1 ± 0.1	65 ± 18	3.5 ± 0.3	52 ± 3
15	5.4 ± 0.1	66 ± 4	5.2 ± 1.2	57 ± 1
16	4.5 ± 1.3	101 ± 1	2.4 ± 0.5	83 ± 6
17	i.a.	i.a.	11.6 ± 3.3	20 ± 5
18	19 ± 8	88 ± 21	32 ± 19	11 ± 3
19	10.3 ± 0.8	38 ± 6	16.4 ± 0.8	24 ± 5
20	i.a.	i.a.	10 ± 1.0	13 ± 3
Wy-14,643	1.6 ± 0.3	100 ± 10	i.a.	i.a.
Pioglitazone	i.a.	i.a.	0.57 ± 0.07	100 ± 6

i.a.: Inactive at tested concentrations (up to 5 or 10 μM). Efficacy values were calculated as the percentage of the maximum obtained fold induction with the reference compounds (Wy-14,643 for PPARα; pioglitazone for PPARγ).

of PPAR activity was observed in the meta-CF_3 analog **7**, whereas the racemate **8**, resulting from the introduction of CF_3 in the ortho position of the phenoxy moiety, displayed very low potency and efficacy on PPARγ and no activity on PPARα.

Next, we examined the activity of derivatives **9**–**17** which were characterized by the presence of F and/or CF_3 either on one of the aromatic rings or both of them while maintaining, with the exception of **17**, the chlorine atom on the para position of the phenoxy moiety. Interestingly, both PPARα and PPARγ activity of most compounds turned out not to be particularly affected, compared to **2**, by the introduction of the substituents. In other words, the electrostatic interaction formed by the chlorine in the receptor pocket seems to be one of the forces driving the binding mode so that any other interaction formed from additional substituents is not able to produce remarkable modifications. In fact, the analog **17**, which was the only compound lacking the chlorine, showed no activity on PPARα and very low potency and efficacy on PPARγ. Moreover, the presence of an additional chlorine on the para position of the benzylic moiety significantly increased the activity; the analog **10**, in fact, was about 3 and 10 times more potent than **2** on PPARα and PPARγ, respectively, while maintaining the same efficacy. Given the relevant activity of this last compound, we decided to prepare and test *S*-**10** which confirmed to be the eutomer displaying approximately a two-fold increase in potency on both PPAR isoforms compared to racemate.

Finally, we decided to test the two analogs **18** and **19** with the aim to evaluate the importance of the benzylic methylene of this series of ligands on PPAR activity. These two compounds, in fact, derived from **9** and **10**, respectively, by removing the methylene unit between the stereogenic center and the phenyl ring. The preference went to these two derivatives due to their high structural similarity with the active metabolite **20** of the selective modulator of PPARγ metaglidasen, which is currently in Phase II clinical development as an oral uricosuric agent for the treatment of hyperuricemia in patients with type 2 diabetes.[34] Even though provided with low potency and efficacy, in vitro and in vivo preclinical studies revealed that metaglidasen has antidiabetic and hypolipidemic activity similar to full agonists without causing some of the typical PPARγ side effects of glitazones. The activity of **18** and **19** turned out to be markedly lower than **9** and **10** on both PPAR isoforms and very similar to that of metaglidasen on PPARγ; however, both analogs showed, differently from metaglidasen,[19] comparable potency and better efficacy on PPARα isotype. The dual PPARα/γ activity of these two newly metaglidasen analogs suggests that they are promising ligands for which a further evaluation of the pharmacological properties in vitro and in vivo could be beneficial.

2.4. Docking studies

To gain more details on the interactions of the most active agonists **6** and *S*-**10** with both PPARγ and PPARα at a molecular level and to propose a binding mode that explains the SAR data, docking experiments were performed into the X-ray crystal structures of both PPARγ complexed with **2** (PDB code: 3CDP) and PPARα complexed with the α/γ dual agonist BMS-631707 (PDB code: 2REW).[37] Ligand docking calculations were performed with the aid of Glide 5.7 in standard precision (SP) mode.[38]

In order to generate a validated docking protocol for the PPAR system, it was necessary to conduct a docking pose validation first. The crystallized conformation of **2** from the receptor/ligand complex structure was utilized for conducting this validation. Ten poses of **2** were generated using the Glide SP mode and re-ranked by GlideScore, Emodel and Glide energy score. The top ranked solution (Fig. 5a and b) for all the three scoring functions was the same and resulted practically identical to the corresponding X-ray pose, as evident from a root-mean-square deviation (rmsd) value of less than 1 Å.

Furthermore, the H-bonds predicted by Glide SP for **2** were virtually identical to those found into the crystallographic PPARγ/**2** complex. Thus, in this study the two ligands **6** and *S*-**10** were docked in both PPARα and PPARγ using the same docking protocol as used in pose validation and the top ranked poses of each ligand based on GlideScore, Emodel and Glide energy score were extracted.

When the ligands were docked into PPARγ, the best scoring trend was observed for Glide energy followed by Emodel and Glide score (Table 2).

Glide energy ranked **2**, **6** and *S*-**10** in the same order as their biological activity with the *S*-**10** pose getting the highest score. The Emodel score ranked *S*-**10** in the first place but **2** was scored higher than **6**. The rank order for GlideScore was the worst wherein the weakest ligand **2** was ranked highest and the most potent *S*-**10** was ranked second. A break up of the Glide energy term showed that the coulombic term (e_{coul}) had a better correlation with the biological activity as compared to the van der Waals term (e_{vdw}). Comparison of the ligand structures shows that the activity of these molecules correlates well with the presence of carboxylate and fluorine groups and corroborates with the docking results, which point towards the importance of the electrostatic interactions. As regards PPARα, the three scoring functions reported in Table 2 showed a different trend. GlideScore ranked **6** and *S*-**10** in the same order as their biological activity with the **6** pose having the highest score. On the contrary, Emodel and Glide energy scores ranked *S*-**10** higher than **6**.

The top ranked poses generated by Glide for **6** and (***S***)-**10** within the PPARγ crystal structure were found to occupy the same spatial position as the crystallized compound **2**. As can be seen in Figure 6, the carboxylate group of both ligands engaged H-bonds with H323, Y473, and H449 side chains involved in the receptor activation, while the substituted-phenoxy and -benzyl moieties were lodged in two hydrophobic pockets, respectively. In particular, the *p*-CF_3-phenoxy ring of **6** and the *o*-F-*p*-Cl-phenoxy ring of *S*-**10** occupied the first cavity of the ligand-binding pocket lined by hydrophobic residues such as F363 of H7, L453, I456 of H11,

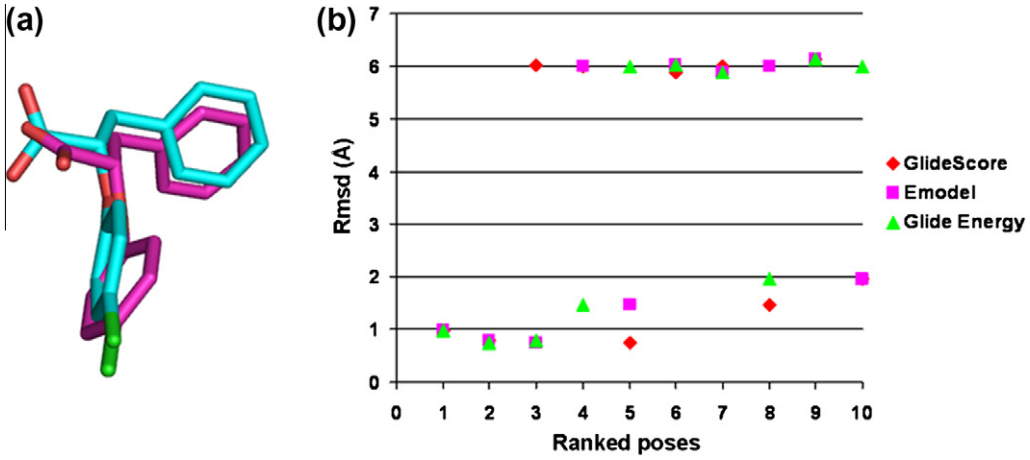

Figure 5. (a) Overlay of the crystallized conformation of **2** (cyan) and the top ranked pose (magenta) based on GlideScore, Emodel and Glide energy score. (b) Plot showing the heavy atom rmsd of the ten poses with the the crystallized conformation of **2** ranked on the basis of GlideScore (red), Emodel (magenta) and Glide energy score (green).

Table 2
Docking scores for the best ranked poses of compounds **2**, **6** and *S*-**10** into PPARγ and **6** and *S*-**10** into PPARα

Compd	EC_{50} (μM)	GlideScore (kcal/mol)	Emodel (kcal/mol)	Glide energy (kcal/mol)	e_{vdw}	e_{coul}
PPARγ						
2	9.6 ± 1.5	−8.42	−47.33	−34.26	−33.66	−0.60
6	0.9 ± 0.2	−7.30	−43.07	−34.51	−30.38	−4.13
S-**10**	0.5 ± 0.2	−7.87	−52.22	−36.15	−31.93	−4.22
PPARα						
6	0.5 ± 0.1	−10.28	−73.22	−43.00	−34.47	−8.53
S-**10**	1.0 ± 0.2	−9.59	−73.50	−46.91	−37.73	−9.18

M463, L465 of the loop 11/12 and F282, C285, Q286 of H3. On the other side, the benzyl ring of **6** and the *p*-Cl-benzyl ring of *S*-**10** were oriented towards the second hydrophobic cavity, interacting with the surrounding amino-acid residues C285 of H3, L330, I326 of H5 and M364 of H7.

Visual inspection of both PPARγ/**6** and PPARγ/*S*-**10** complexes revealed that one *p*-CF_3 fluorine atom of **6** formed a H-bond with the NH_2 group of Q286, while the *o*-F atom of *S*-**10** established a H-bond with the SH group of C285. The F···H–N and F···H–S distance is 2.2 Å for both complexes and the corresponding F···H–N and F···H–S angles are 147.6° and 117.0°, respectively. All these values fall in the range considered acceptable for F···H–X (X = O, N or S) H-bonds.[39] It has been argued that fluorine rarely engages in H-bonds in small molecule X-ray crystal structures.[39] However, in protein pockets where ligands are immobilized by a variety of forces, they appear to be more common. F···X distances beyond 3.0 Å can be regarded as dipole–dipole interactions that most likely provide small stabilizing contributions ($\leqslant$1 kcal mol^{-1}) for the observed binding poses. Our results are consistent with the SAR data showing that **6** and *S*-**10** are the most potent PPARγ ligands of the series with EC_{50} values of 0.9 and 0.5 μM, respectively.

From analysis of docking models we also argued that **6** and *S*-**10**, which have a weak transactivation profile towards PPARγ, preferentially stabilize H3 through closer hydrophobic contacts or H-bonds made with residues of this helix (Q286 and C285). This relationship is in agreement with our previous findings regarding two enantiomeric ureidofibrate-like derivatives complexed with PPARγ, showing partial and full agonism, respectively, towards this nuclear receptor.[40] Even in that case, while the full agonism of one enantiomer could be related to stronger interactions with H11, H12, and the loop 11/12, the partial agonism of the other enantiomer could be ascribed to closer contacts with the residue Q286 of H3.

As depicted in Figure 6, the top ranked poses obtained by Glide for **6** and *S*-**10** were found to dock well also into the PPARα binding site through four H-bonds and many van der Waals contacts. The carboxylate group of the ligands formed a network of H-bond interactions with the residues S280 on H3, Y314 on H5, H440 on H11 and Y464 on H12. H440 was found to engage a further H-bond with the ether oxygen of the two ligands. In addition, the *p*-CF_3-phenoxy ring of **6** and the *o*-F-*p*-Cl-phenoxy ring of *S*-**10** were located in the first binding cavity and made hydrophobic contacts with F351, I354 of H7, V444, I447 of H11, A454 of the loop 11/12 and F273, C276, Q277 of H3. The benzyl ring of **6** and the *p*-Cl-benzyl ring of *S*-**10** fitted into the second hydrophobic cavity formed by residues T279, C276 of H3, I317, F318 L321 of H4, M330 of β-sheet, and M355 of H7.

3. Conclusions

In conclusion, we prepared and tested a new series of fluorinated analogs of the previously reported PPAR α/γ dual agonist **2**. The displacement of the chlorine atom of this ligand generally resulted in compounds with lower potency and efficacy on both isoforms, whereas the introduction of additional fluorine or CF_3 into the molecular structure of **2** did not markedly affect the activity. This allows to hypothesize that the electrostatic interactions made from chlorine with PPAR residues, as seen in the X-ray structure of the complex PPARγ/**2**, are determinant for agonist activity. Only the substitution of chlorine with CF_3 or the introduction of an additional fluorine in the ortho position of aryloxy ring of **2** afforded significantly more potent and effective agonists and docking experiments were performed to rationalize this peculiar behavior. The presence of the methylene unit between the stereogenic center and the phenyl ring of **2** also turned out to be important for

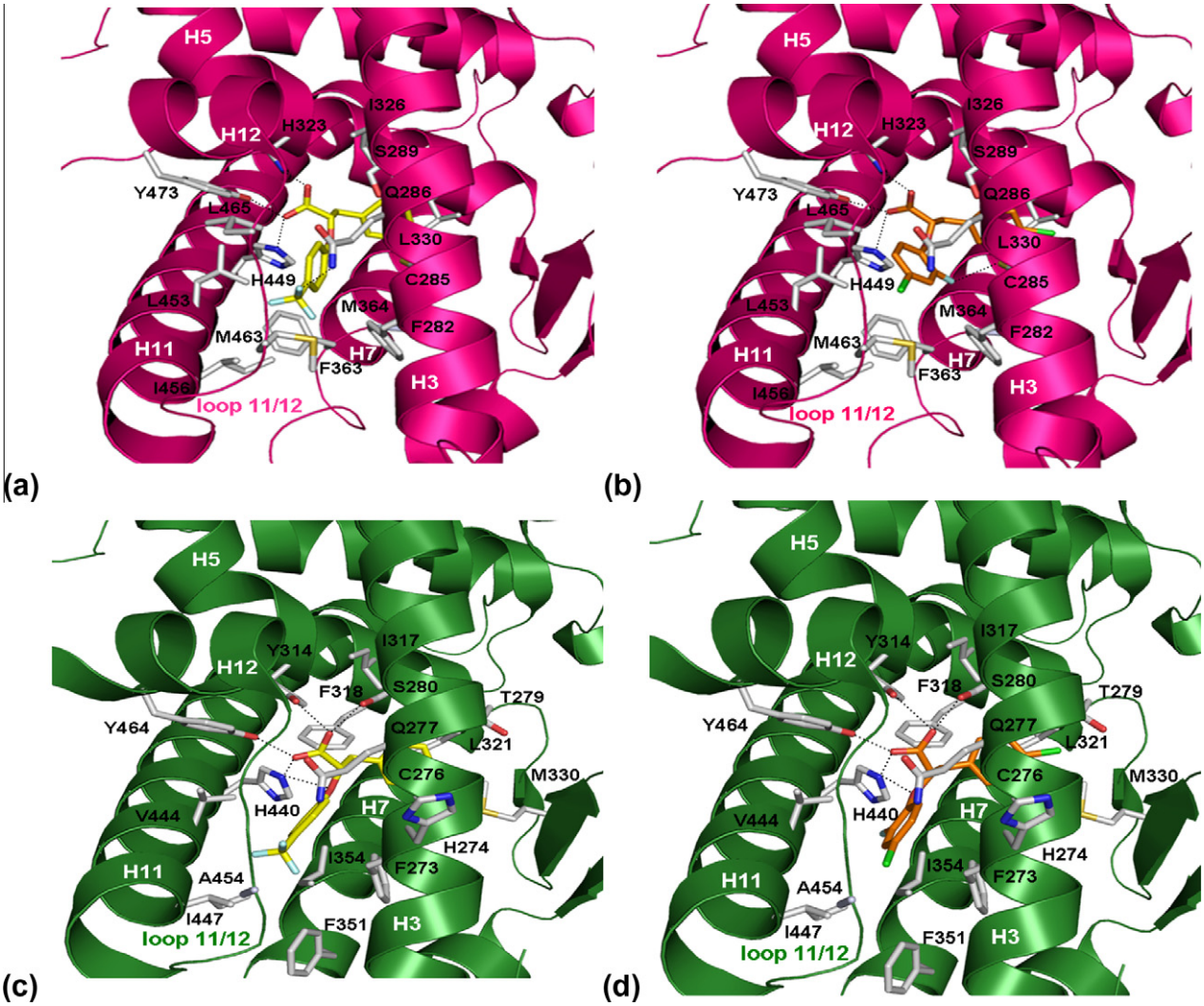

Figure 6. Compounds **6** (a, yellow) and *S*-**10** (b, orange) docked into the PPARγ binding site are represented as a slate hot pink ribbon model. Compounds **6** (c) and *S*-**10** (d) docked into the PPARα binding site are represented as a green ribbon model. Only amino acids directly implicated in the ligand binding are displayed (white) and labeled. H-bonds discussed in the text are depicted as dashed black lines.

activity. Its removal, in fact, decreased potency and efficacy as shown by derivatives **18** and **19** having high structural similarity with the active metabolite of metaglidasen. Differently from metaglidasen, however, both these analogs showed a PPAR α/γ dual activity which makes them promising ligands for which a further evaluation of the pharmacological properties in vitro and in vivo could be beneficial.

4. Experimental section

4.1. Protein expression, purification and crystallization

The LBD of PPARγ was expressed as N-terminal His-tagged protein using a pET28 vector and purified as previously described.[40] Crystals of apo-PPARγ were obtained by vapor diffusion at 20 °C using sitting drop made by mixing 2 μL of protein solution (15 mg mL^{-1}, in 20 mM Tris, 5 mM DTT, 0.5 mM EDTA, pH 8.0) with 2 μL of reservoir solution (0.8 M NaCitrate, 0.15 mM Tris, pH 8.0). The crystals were soaked for 7 days in a storage solution (1.2 M NaCitrate, 0.15 M Tris, pH 8.0) containing the ligands (0.1 mM). The ligands were dissolved in ethanol and diluted in the storage solution so that the final ethanol concentration was 0.5%. The storage solution with 20% glycerol (v/v) was used as cryoprotectant. Crystals of PPARγ/**2** belong to the space group C2 with cell parameters shown in Table 1 of the Supplementary data. The asymmetric unit is formed by one homodimer.

4.2. Structure determination

X-ray data were collected at 100 K under a nitrogen stream using synchrotron radiation (beamline ID14-1 at ESRF, Grenoble). The diffracted intensities were processed using the programs MOSFLM and SCALA.[41] Refinements were performed with CNS[42] using the coordinates of apo-PPARγ (PDB code 1PRG) as a starting model.[43] All data between 8 and 2.8 Å were included in the refinement. The statistics of crystallographic data and refinement are summarized in Table 1 of the Supplementary data. The coordinates of PPARγ/**2** complex have been deposited in the Brookhaven Protein Data Bank (PDB) with the code 3CDP.

4.3. Computational resources

Molecular modeling and graphics manipulations were performed using Maestro 9.2[44] running on a Linux workstation with an Intel Core i7 920 CPU and 12 GB of RAM. Glide 5.7[38] was used

for all docking calculations. Figures were generated using Pymol 1.0.[45]

4.4. Ligand and receptor preparation

Molecular models of compounds **2**, **6** and *S*-**10** were built and minimized with the Maestro module of the Schrödinger molecular modeling package. The Polak–Ribiere conjugate gradient (PRCG) method with a 0.001 kcal mol^{-1} $Å^{-1}$ convergence threshold was used for the geometry optimization calculations. These structures were then incorporated into the LigPrep 2.5 module of Schrödinger.[46] The protonation state for all ionizable groups was set at neutral pH 7.

The crystal structures of PPARγ in complex with **2** (PDB code: 3CDP) and of PPARα in complex with the α/γ dual agonist BMS-631707 (PDB code: 2REW)[37] were prepared using the 'Protein Preparation Wizard' panel of Schrödinger molecular modeling package. In particular, using the 'preprocess and analyze structure' tool, the bond orders were assigned, all the hydrogen atoms were added, the bound ligand and all the water molecules were deleted. Using Epik 2.2,[47] a prediction of the heterogroups ionization and tautomeric states was performed. An optimization of the H-bonding network was performed using the 'H-bond assignment' tool. Finally, using the 'impref utility', the positions of the hydrogen atoms were optimized by keeping all the heavy atoms in place.

4.5. Docking simulations

2, **6** and *S*-**10** were docked into both PPARγ and PPARα binding sites using the Glide 5.7 program in SP mode.[38,48] The binding region was defined by a 10 × 10 × 10 Å box centered on the crystallized conformation of ligand **2** for PPARγ and BMS-631707 for PPARα. A scaling factor of 0.8 was applied to the van der Waals radii. Default settings were used for all the remaining parameters. Ten poses were generated for each ligand and re-ranked using the scoring terms available in Glide.

4.6. Biological methods

Medium, other cell culture reagents, pioglitazone and Wy-14,643 were purchased from Sigma (Milan, Italy). The active metabolite of metaglidasen was synthesized in-house.

4.7. Plasmids

The expression vectors expressing the chimeric receptors containing the yeast GAL4-DNA binding domain fused to either the human PPARα/PPARγ ligand binding domain (LBD) and the reporter plasmid for these GAL4 chimeric receptors (pGAL5TKpGL3) containing five repeats of the GAL4 response elements upstream of a minimal thymidine kinase promoter that is adjacent to the luciferase gene were described previously.[49]

4.8. Cell culture and transfections

Human hepatoblastoma cell line HepG2 (Interlab Cell Line Collection, Genoa, Italy) was cultured in Minimum Essential Medium (MEM) containing 10% of heat inactivated Foetal Bovine Serum, 100 U penicillin G mL^{-1} and 100 μg streptomycin sulfate mL^{-1} at 37 °C in a humidified atmosphere of 5% CO_2. For transactivation assay 10^5 cells/well were seeded in a 24-well plate in triplicate and transfections were performed after 24 h, with the CAPHOS® (Sigma, Milan, Italy), a calcium–phosphate method, according to the manufacturer guidelines. Cells were transfected with expression plasmids encoding the fusion protein GAL4-PPARα LBD or GAL4-PPARγ LBD (30 ng), pGAL5TKpGL3 (100 ng), pCMVβgal (250 ng). After transfection, cells were treated for 20 h with the indicated ligands. Luciferase activity in cell extracts was then determined by a luminometer (VICTOR^3 V Multilabel Reader, PerkinElmer). β-Galactosidase activity was determined using β-D-galactopyranoside (Sigma, Milan, Italy) as described previously.[50] All transfection experiments were repeated at least twice.

4.9. Chemical methods

Column chromatography was performed on ICN Silica Gel 60 Å (63–200 μm) as a stationary phase. Melting points were determined in open capillaries on a Gallenkamp electrothermal apparatus and are uncorrected. Mass spectra were recorded on an HP GC/MS 6890-5973 MSD spectrometer, electron impact 70 eV, equipped with HP chemstation or an Agilent LC/MS 1100 Series LC/MSD Trap System VL spectrometer, electrospray ionization (ESI). ^{1}H NMR spectra were recorded in $CDCl_3$ (the use of other solvents is specified) on a Varian-Mercury 300 (300 MHz) spectrometer. Chemical shifts are expressed as parts per million (ppm, δ). Microanalyses of solid compounds were carried out with an Eurovector Euro EA 3000 model analyzer; the analytical results are within ±0.4% of theoretical values. Only for final compounds **3**, **4**, **9**, **18** and **19** the data related to carbon are 0.64%, −0.85%, 0.74%, 0.67% and 0.72%, respectively.

Optical rotations were measured with a Perkin-Elmer 341 polarimeter at room temperature (20 °C): concentrations are expressed as g 100 mL^{-1}. The CD curves were registered on a J-810 model JASCO spectropolarimeter. The enantiomeric excesses of acids were determined by HPLC analysis of acids or their methyl esters, obtained by reaction with an ethereal solution of diazomethane, on Chiralcel OD or AD columns (4.6 mm i.d. × 250 mm, Daicel Chemical Industries, Ltd, Tokyo, Japan). Analytical liquid chromatography was performed on a PE chromatograph equipped with a Rheodyne 7725i model injector, a 785A model UV/vis detector, a series 200 model pump and NCI 900 model interface. Chemicals were from Aldrich (Milan, Italy), Lancaster (Milan, Italy) or Across (Milan, Italy) and were used without any further purification.

4.10. Preparation of ethyl 2-aryloxy-3-phenylpropanoates

4.10.1. General procedure

To an ice-bath cooled suspension of Ph_3P–PS (2% DVB, 3 mmol g^{-1}, 13.8 mmol) in anhydrous toluene (35 mL) was added dropwise a solution of diisopropylazodicarboxylate (DIAD, 13.5 mmol) in anhydrous toluene (35 mL). The resulting mixture was stirred for 0.5 h. A solution of racemic or (*R*)-ethyl phenyllactate (11 mmol) in anhydrous toluene (50 mL) and corresponding phenol (10 mmol) was added at room temperature. The reaction mixture was stirred overnight at rt, under N_2 atmosphere. The solid was filtered off and the filtrate was evaporated to dryness. The residue was chromatographed on silica gel column (petroleum ether/ethyl acetate 9:1 or 8:2 as eluent), affording the desired compounds as pale yellow oils in 58–92% yields.

4.10.2. (*S*)-Ethyl 2-(4-fluoro-phenoxy)-3-phenylpropanoate

78% yield; ^{1}H NMR: δ = 1.18 (t, 3H, CH_3CH_2O), 3.21–3.23 (m, 2H, $PhCH_2$), 4.17 (q, 2H, CH_3CH_2O), 4.68–4.72 (m, 1H, CH), 6.74–6.79, 6.88–6.94 and 7.22–7.32 (m, 9H, aromatics); GC/MS, *m*/*z* (%): 288 (83) $[M]^+$, 215 (30), 177 (100).

4.10.3. Ethyl 2-(3-fluoro-phenoxy)-3-phenylpropanoate

76% yield; ^{1}H NMR: δ = 1.19 (t, 3H, CH_3CH_2O), 3.22–3.25 (m, 2H, $PhCH_2$), 4.17 (q, 2H, CH_3CH_2O), 4.74–4.78 (m, 1H, CH), 6.54–6.78 and 7.13–7.31 (m, 9H, aromatics); GC/MS, *m*/*z* (%): 288 (35) $[M]^+$, 215 (38), 177 (100).

4.10.4. Ethyl 2-(2-fluoro-phenoxy)-3-phenylpropanoate

92% yield; ^{1}H NMR: δ = 1.18 (t, 3H, CH_3CH$_2$O), 3.23–3.30 (m, 2H, PhCH$_2$), 4.17 (q, 2H, CH$_3$CH_2O), 4.77–4.82 (m, 1H, CH), 6.78–7.08 and 7.24–7.33 (m, 9H, aromatics); GC/MS, *m*/*z* (%): 288 (33) [M]$^+$, 215 (22), 177 (100).

4.10.5. (*S*)-Ethyl 2-(3-trifluoromethyl-phenoxy)-3-phenylpropanoate

70% yield; ^{1}H NMR: δ = 1.19 (t, 3H, CH_3CH$_2$O), 3.22–3.32 (m, 2H, PhCH$_2$), 4.11–4.23 (m, 2H, CH$_3$CH_2O), 4.79–4.84 (m, 1H, CH), 6.97–7.06 and 7.19–7.37 (m, 9H, aromatics); GC/MS, *m*/*z* (%): 338 (11) [M]$^+$, 177 (100), 135 (47), 105 (32).

4.10.6. Ethyl 2-(2-trifluoromethyl-phenoxy)-3-phenylpropanoate

58% yield; ^{1}H NMR: δ = 1.14 (t, 3H, CH_3CH$_2$O), 3.25–3.34 (m, 2H, PhCH$_2$), 4.14 (q, 2H, CH$_3$CH_2O), 4.87–4.91 (m, 1H, CH), 6.74–7.02, 7.21–7.41 and 7.55–7.58 (m, 9H, aromatics); GC/MS, *m*/*z* (%): 338 (6) [M]$^+$, 177 (100), 135 (56).

4.10.7. (*S*)-Ethyl 2-(4-chloro-2-fluoro-phenoxy)-3-phenylpropanoate

59% yield; ^{1}H NMR: δ = 1.19 (t, 3H, CH_3CH$_2$O), 3.21–3.34 (m, 2H, PhCH$_2$), 4.17 (q, 2H, CH$_3$CH_2O), 4.73–4.78 (m, 1H, CH), 6.70–6.75, 6.91–6.97, 7.04–7.09 and 7.21–7.32 (m, 8H, aromatics); GC/MS, *m*/*z* (%): 324 (8) [M+2]$^+$, 322 (25) [M]$^+$, 177 (100), 135 (87).

4.10.8. Ethyl 2-(4-chloro-3-fluoro-phenoxy)-3-phenylpropanoate

92% yield; ^{1}H NMR: δ = 1.19 (t, 3H, CH_3CH$_2$O), 3.23 (d, 2H, PhCH$_2$), 4.19 (q, 2H, CH$_3$CH_2O), 4.72 (t, 1H, CH), 6.54–6.67 and 7.19–7.32 (m, 8H, aromatics); GC/MS, *m*/*z* (%): 324 (15) [M+2]$^+$, 322 (47) [M]$^+$, 177 (100), 105 (68).

4.10.9. Ethyl 2-(4-chloro-3-trifluoromethyl-phenoxy)-3-phenylpropanoate

61% yield; ^{1}H NMR: δ = 1.20 (t, 3H, CH_3CH$_2$O), 3.25 (d, 2H, PhCH$_2$), 4.25 (m, 2H, CH$_3$CH_2O), 4.77 (d, 1H, CH), 6.87–7.01, 7.14–7.15 and 7.23–7.35 (m, 8H, aromatics); GC/MS, *m*/*z* (%): 374 (8) [M+2]$^+$, 372 (24) [M]$^+$, 177 (100), 135 (69), 105 (46).

4.11. Preparation of diethyl 2-aryloxy-malonates

4.11.1. General procedure

A mixture of diethyl chloromalonate (19.1 mmol) and suitable sodium phenate (20.1 mmol), prepared from an equivalent amount of the corresponding phenol and sodium in abs EtOH, was stirred and heated under reflux in acetone (100 mL) for 4 h. The solvent was removed under reduced pressure, the residue was taken up with water and extracted with ethyl acetate. The combined organic extracts were washed with brine, dried over Na_2SO_4 and concentrated to give an oily residue which was chromatographed on silica gel column (petroleum ether/ethyl acetate 9:1 as eluent). The desired compounds were obtained as pale yellow oils in 14–77% yield.

4.11.2. Diethyl 2-(4-chloro-phenoxy)malonate

77% yield; ^{1}H NMR: δ = 1.29 (t, 6H, 2CH$_3$), 4.30 (q, 4H, 2CH$_2$), 5.14 (s, 1H, CH), 6.80–7.26 (m, 4H, aromatics); GC/MS, *m*/*z* (%): 288 (34) [M+2]$^+$, 286 (100) [M]$^+$, 141 (89).

4.11.3. Diethyl 2-(2-fluoro-4-chloro-phenoxy)malonate

58% yield; ^{1}H NMR: δ = 1.30 (t, 6H, 2CH$_3$), 4.31 (q, 4H, 2CH$_2$), 5.15 (s, 1H, CH), 6.99–7.16 (m, 3H, aromatics); GC/MS, *m*/*z* (%): 306 (21) [M+2]$^+$, 304 (62) [M]$^+$, 231 (17), 159 (100), 147 (32).

4.11.4. Diethyl 2-(2-trifluoromethyl-phenoxy)malonate

14% yield; ^{1}H NMR: δ = 1.30 (t, 6H, 2CH$_3$), 4.32 (q, 4H, 2CH$_2$), 5.22 (s, 1H, CH), 6.88–6.91, 7.08–7.13, 7.44–7.50 and 7.61–7.64 (m, 4H, aromatics); GC/MS, *m*/*z* (%): 320 (44) [M]$^+$, 200 (36), 171 (100), 143 (37).

4.12. Preparation of diethyl 2-aryloxy-2-benzyl-malonates

4.12.1. General procedure

A solution of the suitable diethyl aryloxy-malonate,[36] (10 mmol) in anhydrous DMF (25 mL) was added dropwise to a suspension of NaH (95% powder, 18 mmol) in anhydrous DMF (20 mL) at 0 °C. After stirring for 20 min at rt, a solution of the suitable substituted benzylbromide (12 mmol) in anhydrous DMF (15 mL) was added dropwise and the resulting reaction mixture stirred at 60 °C for 15–20 h. The solvent was removed under reduced pressure and the residue poured into water and extracted with diethyl ether. The organic layer was washed with saturated ammonium chloride solution, dried over Na_2SO_4 and the solvent evaporated in vacuo to give an oily residue which was chromatographed on silica gel column (petroleum ether/ethyl acetate 95:5 as eluent). The title compounds were obtained as pale yellow oils in 30–45% yields.

4.12.2. Diethyl 2-(2-fluoro-4-chloro-phenoxy)-2-(4-chloro-benzyl)-malonate

35% yield; ^{1}H NMR: δ = 1.15 (t, 6H, 2CH_3CH$_2$O), 3.53 (s, 2H, ArCH$_2$), 4.15 (q, 4H, 2CH$_3$CH_2O), 6.93–7.26 (m, 7H, aromatics); GC/MS, *m*/*z* (%): 432 (2) [M+4]$^+$, 430 (11) [M+2]$^+$, 428 (17) [M]$^+$, 283 (29), 237 (100).

4.12.3. Diethyl 2-(4-chloro-phenoxy)-2-(2-fluoro-benzyl)-malonate

35% yield; ^{1}H NMR: δ = 1.15 (t, 6H, 2CH_3CH$_2$O), 3.67 (s, 2H, ArCH$_2$), 4.18 (q, 4H, 2CH$_3$CH_2O), 6.83–7.27 (m, 8H, aromatics); GC/MS, *m*/*z* (%): 396 (29) [M+2]$^+$, 394 (83) [M]$^+$, 221 (100).

4.12.4. Diethyl 2-(4-chloro-phenoxy)-2-(3-fluoro-benzyl)-malonate

30% yield; ^{1}H NMR: δ = 1.16 (t, 6H, 2CH_3CH$_2$O), 3.67 (s, 2H, ArCH$_2$), 4.17 (q, 4H, 2CH$_3$CH_2O), 6.71–6.89 and 7.16–7.19 (m, 8H, aromatics); GC/MS, *m*/*z* (%): 396 (32) [M+2]$^+$, 394 (90) [M]$^+$, 321 (49), 221 (100).

4.12.5. Diethyl 2-(4-chloro-phenoxy)-2-(4-fluoro-benzyl)-malonate

45% yield; ^{1}H NMR: δ = 1.14 (t, 6H, 2CH_3CH$_2$O), 3.55 (s, 2H, ArCH$_2$), 4.16 (q, 4H, 2CH$_3$CH_2O), 6.81–6.99 and 7.12–7.26 (m, 8H, aromatics); GC/MS, *m*/*z* (%): 396 (19) [M+2]$^+$, 394 (51) [M]$^+$, 221 (100).

4.12.6. Diethyl 2-(2-fluoro-4-chloro-phenoxy)-2-(3-fluoro-benzyl)-malonate

37% yield; ^{1}H NMR: δ = 1.15 (t, 6H, 2CH_3CH$_2$O), 3.56 (s, 2H, ArCH$_2$), 4.16 (q, 4H, 2CH$_3$CH_2O), 6.93–7.13 and 7.20–7.26 (m, 7H, aromatics); GC/MS, *m*/*z* (%): 414 (18) [M+2]$^+$, 412 (51) [M]$^+$, 221 (100).

4.12.7. Diethyl 2-(2-trifluoromethyl-phenoxy)-2-(3-fluoro-benzyl)-malonate

36% yield; ^{1}H NMR: δ = 1.08 (t, 6H, 2CH_3CH$_2$O), 3.59 (s, 2H, ArCH$_2$), 4.13 (q, 4H, 2CH$_3$CH_2O), 6.91–7.39 and 7.59–7.62 (m, 8H, aromatics); GC/MS, *m*/*z* (%): 428 (7) [M]$^+$, 221 (100).

4.12.8. Preparation of ethyl 2-(4-chloro-2-fluoro-phenoxy)-2-arylacetates

Sodium 4-chloro-2-fluoro-phenate (12 mmol) was dissolved in abs. EtOH (30 mL) and added dropwise to a solution of ethyl 2-bromo-2-arylethanoate (10 mmol) in abs. EtOH (90 mL). The resulting mixture was refluxed for 24 h and the solvent was evaporated to dryness. The resulting residue was dissolved in ethyl acetate, washed twice with 0.5 N NaOH and brine, dried over Na_2SO_4 and the solvent was evaporated to dryness affording a yellow oil residue. The desired compounds were obtained as colorless oily by column chromatography on silica gel using petroleum ether/ethyl acetate 98:2 as eluent.

4.12.9. Ethyl 2-(4-chloro-2-fluoro-phenoxy)-2-phenylacetate

43% yield; ^{1}H NMR: δ = 1.20 (t, 3H, C*H*$_3$CH$_2$O), 4.20 (q, 2H, CH$_3$C*H*$_2$O), 5.60 (s, 1H, CH), 6.85–7.01, 7.10–7.14, 7.34–7.43 and 7.53–7.57 (m, 8H, aromatics); GC/MS, *m*/*z* (%): 310 (3) $[M+2]^+$, 308 (9) $[M]^+$, 163 (100).

4.12.10. Ethyl 2-(4-chloro-2-fluoro-phenoxy)-2-(4-chloro-phenyl)acetate

46% yield; ^{1}H NMR: δ = 1.20 (t, 3H, C*H*$_3$CH$_2$O), 4.21 (m, 2H, CH$_3$C*H*$_2$O), 5.57 (s, 1H, CH), 6.84–7.14 and 7.33–7.52 (m, 7H, aromatics); GC/MS, *m*/*z* (%): 346 (1) $[M+4]^+$, 344 (3) $[M+2]^+$, 342 (4) $[M]^+$, 269 (26), 197 (100).

4.13. Preparation of the final acids 3–5, 7–9, 11, 12, 18 and 19

4.13.1. General procedure

To a stirred solution of the corresponding ethyl ester (1 mmol) in THF (10 mL) was added 2 N NaOH (10 mL). The reaction mixture was stirred for 4–8 h. THF was evaporated in vacuo and the aqueous phase was acidified with 2 N HCl and extracted with Et_2O. The combined organic layers were washed twice with brine, dried over Na_2SO_4 and evaporated to dryness affording the title acids, except for **4**, as white solids, which were recrystallized from *n*-hexane or $CHCl_3$/*n*-hexane.

The acid **4**, obtained as a colorless oil, was dissolved in 95% EtOH (10 mL) and added with a solution of $NaHCO_3$ (1 equiv) in H_2O (1 mL). The reaction mixture was stirred for 2 h and then the solvent was evaporated to dryness affording the corresponding sodium salt as a white solid which was recrystallized from MeOH/$CHCl_3$.

4.13.2. (*S*)-2-(4-Fluoro-phenoxy)-3-phenylpropanoic acid (3)

98% yield (*n*-hexane); mp: 85–86 °C; $[\alpha]_D$ +19 (*c* 1.0 in MeOH); ^{1}H NMR: δ = 3.20–3.33 (m, 2H, CH$_2$), 4.76–4.80 (m, 1H, CH), 6.75–6.81, 6.89–6.96 and 7.24–7.34 (m, 10H, 9 aromatics + COOH, D_2O exchanged); GC/MS, *m*/*z* (%) (methyl ester): 274 (41) $[M]^+$, 163 (52), 121 (100); ee >99% (HPLC, methyl ester: Chiralcel OD column, *n*-hexane/*i*-propanol 95:5, flow rate 1 mL min^{-1}, detection 280 nm); Anal. Calcd for $C_{15}H_{13}FO_3$: C, 69.22; H, 5.03. Found: C, 69.86; H, 5.09.

4.13.3. Sodium 2-(3-Fluoro-phenoxy)-3-phenylpropanoate (4)

99% yield; mp: 250 °C dec.; ^{1}H NMR: δ = 3.10–3.23 (m, 2H, CH$_2$), 4.49–4.53 (m, 1H, CH), 6.53–6.65 and 7.10–7.35 (m, 9H, aromatics); Anal. Calcd for $C_{15}H_{12}FO_3Na$: C, 63.83; H, 4.29. Found: C, 62.98; H, 4.21.

4.13.4. 2-(2-Fluoro-phenoxy)-3-phenylpropanoic acid (5)

58% yield ($CHCl_3$/*n*-hexane); mp: 90–91 °C; ^{1}H NMR: δ = 3.24–3.37 (m, 2H, CH$_2$), 4.83–4.88 (m, 1H, CH), 6.75–6.83, 6.90–7.10 and 7.22–7.36 (m, 10H, 9 aromatics + COOH, D_2O exchanged); GC/MS, *m*/*z* (%) (methyl ester): 274 (14) $[M]^+$, 163 (65), 121 (100); Anal. Calcd for $C_{15}H_{13}FO_3$: C, 69.22; H, 5.03. Found: C, 69.57; H, 5.02.

4.13.5. (*S*)-2-(3-Trifluoromethyl-phenoxy)-3-phenylpropanoic acid (7)

88% yield (*n*-hexane); mp: 62–64 °C; $[\alpha]_D$ −22 (*c* 1.0 in MeOH); ^{1}H NMR: δ = 3.24–3.37 (m, 2H, CH$_2$), 4.87–4.91 (m, 1H, CH), 6.91–7.07 and 7.17–7.39 (m, 10H, 9 aromatics + COOH, D_2O exchanged); ESI-MS *m*/*z* (%) negative: 309 (100) $[M-H]^{-1}$, 161 (55), 147 (8); ee >99% (HPLC: Chiralcel OD column; hexane/*i*-propanol/TFA 95:5:0.05, flow rate 1 mL min^{-1}, detection 254 nm); Anal. Calcd for $C_{16}H_{13}F_3O_3$: C, 61.94; H, 4.22. Found: C, 62.34; H, 4.28.

4.13.6. 2-(2-Trifluoromethyl-phenoxy)-3-phenylpropanoic acid (8)

84% yield ($CHCl_3$/*n*-hexane); mp: 210–212 °C; ^{1}H NMR (DMSO-d_6): δ = 2.93–3.24 (m, 2H, CH$_2$), 4.43–4.47 (m, 1H, CH), 6.87–6.92, 7.09–7.28 and 7.38–7.47 (m, 10H, 9 aromatics + COOH, D_2O exchanged); ESI-MS *m*/*z* (%) negative: 309 (94) $[M-H]^{-1}$, 161 (100), 147 (5); Anal. Calcd for $C_{16}H_{13}F_3O_3$: C, 61.94; H, 4.22. Found: C, 61.88; H, 4.22.

4.13.7. (*S*)-2-(4-Chloro-2-fluoro-phenoxy)-3-phenylpropanoic acid (9)

95% yield ($CHCl_3$/*n*-hexane); mp: 88–89 °C; $[\alpha]_D$ −20 (*c* 1.0 in MeOH); ^{1}H NMR: δ = 3.23–3.36 (m, 2H, CH$_2$), 4.79–4.83 (m, 1H, CH), 5.10 (bb, 1H, COOH, D_2O exchanged), 6.68–6.74, 6.91–6.97, 7.05–7.10 and 7.23–7.35 (m, 8H, aromatics); GC/MS, *m*/*z* (%) (methyl ester): 310 (9) $[M+2]^+$, 308 (27) $[M]^+$, 163 (70), 121 (100); ee >99% (HPLC: Chiralcel AD column, hexane/*i*-propanol/TFA 95:5:0.02, flow rate 1 mL min^{-1}, detection 254 nm); Anal. Calcd for $C_{15}H_{12}ClFO_3$: C, 61.13; H, 4.10. Found: C, 61.87; H, 4.07.

4.13.8. 2-(4-Chloro-3-fluoro-phenoxy)-3-phenylpropanoic acid (11)

96% yield ($CHCl_3$/*n*-hexane); mp: 116–117 °C; ^{1}H NMR: δ = 3.21–3.34 (m, 2H, CH$_2$), 4.76–4.80 (m, 1H, CH), 5.51 (bb, 1H, COOH, D_2O exchanged), 6.55–6.67 and 7.20–7.34 (m, 8H, aromatics); GC/MS, *m*/*z* (%) (methyl ester): 310 (6) $[M+2]^+$, 308 (18) $[M]^+$, 163 (31), 121 (100); Anal. Calcd for $C_{15}H_{12}ClFO_3$: C, 61.13; H, 4.10. Found: C, 60.87; H, 4.03.

4.13.9. 2-(4-Chloro-3-trifluoromethyl-phenoxy)-3-phenylpropanoic acid (12)

85% yield ($CHCl_3$/*n*-hexane); mp: 78–79 °C; ^{1}H NMR: δ = 3.23–3.37 (m, 2H, CH$_2$), 4.82–4.87 (m, 1H, CH), 6.87–6.91, 7.14–7.15 and 7.20–7.36 (m, 9H, 8 aromatics + COOH, D_2O exchanged); ESI-MS *m*/*z* (%) negative: 345 (3) $[M+2-H]^{-1}$, 343 (10) $[M-H]^{-1}$, 195 (100); Anal. Calcd for $C_{16}H_{12}ClF_3O_3$: C, 55.75; H, 3.51. Found: C, 55.87; H, 3.57.

4.13.10. 2-(4-Chloro-2-fluoro-phenoxy)phenylacetic acid (18)

98% yield ($CHCl_3$/*n*-hexane); mp: 110–111 °C; ^{1}H NMR: δ = 5.63 (s, 1H, CH), 6.84–6.90, 6.96–7.00, 7.10–7.14, 7.34–7.44 and 7.52–7.56 (m, 9H, 8 aromatics + COOH, D_2O exchanged); ESI-MS *m*/*z* (%) negative: 281 (13) $[M+2-H]^{-1}$, 279 (40) $[M-H]^{-1}$, 235 (3), 129 (100); Anal. Calcd for $C_{14}H_9FClO_3$: C, 59.91; H, 3.59. Found: C, 60.58; H, 3.69.

4.13.11. 2-(4-Chloro-2-fluoro-phenoxy)-2-(4-chloro-phenyl)acetic acid (19)

99% yield (*n*-hexane); mp: 110–12 °C; ^{1}H NMR: δ = 4.57 (bb, 1H, COOH, D_2O exchanged), 5.61 (s, 1H, CH), 6.84–6.89, 6.98–7.02, 7.11–7.16, 7.36–7.42 and 7.47–7.54 (m, 7H, aromatics); ESI-MS *m*/*z* (%) negative: 317 (11) $[M+4-H]^{-1}$, 315 (64) $[M+2-H]^{-1}$, 313

(100) $[M-H]^{-1}$, 269 (31), 129 (57); Anal. Calcd for $C_{14}H_8FCl_2O_3$: C, 53.36; H, 2.88. Found: C, 54.08; H, 3.00.

4.13.12. Preparation of pantolactone esters of 10

(*R*)-Pantolactone (12 mmol), dimethylaminopyridine (DMAP, 0.1 mmol) and 1,3-dicyclohexylcarbodiimide (DCC, 10 mmol) were added, under N_2 atmosphere, to a stirred solution of the racemic acid **10** (12 mmol) in anhydrous THF (50 mL). The reaction mixture was stirred at room temperature for 48 h, afterwards the precipitate was filtered off and the organic phase was evaporated to dryness. The mixture of diastereomeric esters was obtained, as a white solid, by column chromatography on silica gel using petroleum ether/ethyl acetate 95:5 as eluent. The recrystallization of the mixture from $CHCl_3$/*n*-hexane 1:7 afforded the desired (*S*,*R*)-diastereomer.

4.13.13. (*R*)-Pantolactone ester of (*S*)-2-(4-chloro-2-fluoro-phenoxy)-3-(4-chloro-phenyl)propanoic acid

13% yield; ^{1}H NMR: δ = 0.93 and 1.03, (s, 6H, CHC(CH_3)$_2$, major diastereomer), 3.26–3.40 (m, 2H, CHCH_2), 3.97–4.05 (m, 2H, CH_2O-CO), 4.87–4.91 (m, 1H, ArOC*H*COO), 5.35 (s, 1H, C*H*C(CH_3)$_2$), 6.82–6.88, 6.99–7.12 and 7.27–7.37 (m, 7H, aromatics); GC/MS, *m*/*z* (%): 444 (1) $[M+4]^+$, 442 (7) $[M+2]^+$, 440 (10) $[M]^+$, 295 (49), 165 (100); de = 99% as determined by comparing the signals integrations of the methyls of the pantolactone moiety (δ = 0.96 and 1.10 for the minor diastereomer).

4.14. Preparation of the final acids 10, *S*-10 and 13–17

4.14.1. General procedure

The suitable diethyl malonate (3 mmol), obtained from the reaction described above, was refluxed under stirring with 1 N NaOH (3 mL) in 95% EtOH (12 mL) for 4–6 h. The organic solvent was distilled off under reduced pressure and the resulting aqueous phase washed with Et_2O, acidified to pH 2 with 6 N HCl and extracted with Et_2O. The combined organic extracts were dried over Na_2SO_4 and the solvent removed under reduced pressure. The resulting mixture was heated at 160 °C for 2 h affording the desired acids as white solids which were purified by recrystallization from *n*-hexane/$CHCl_3$.

4.14.2. 2-(4-Chloro-2-fluoro-phenoxy)-3-(4-chloro-phenyl)propanoic acid (10)

82% yield; mp: 132–134 °C; ^{1}H NMR: δ = 3.20–3.33 (m, 2H, CH_2), 4.77–4.81 (m, 1H, CH), 6.72–6.78, 6.96–7.00, 7.07–7.11 and 7.23–7.30 (m, 8H, 7 aromatics + COOH, D_2O exchanged); ESI-MS *m*/*z* (%) negative: 327 (53) $[M-H]^{-1}$, 181 (54), 145 (100); Anal. Calcd for $C_{15}H_{11}Cl_2FO_3$: C, 54.74; H, 3.37. Found: C, 54.98; H, 3.42.

4.14.3. (*S*)-2-(4-Chloro-2-fluoro-phenoxy)-3-(4-chloro-phenyl)propanoic acid [*S*-10]

99% yield; mp: 86–88 °C; $[\alpha]_D$ −6 (*c* 1.0 in MeOH); ee >99% (HPLC: Chiralcel AD column; hexane/*i*-propanol/TFA 99:1:0.04; flow rate 1 mL min^{-1}; detection 254 nm); Anal. Calcd for $C_{15}H_{11}Cl_2FO_3$: C, 54.74; H, 3.37. Found: C, 54.41; H, 3.37.

4.14.4. 2-(4-Chloro-phenoxy)-3-(2-fluoro-phenyl)propanoic acid (13)

55% yield; mp: 113–114 °C; ^{1}H NMR: δ = 3.23–3.42 (m, 2H, CH_2), 4.82–4.87 (m, 1H, CH), 6.73–6.78, 6.91–7.10 and 7.17–7.32 (m, 9H, 8 aromatics + COOH, D_2O exchanged); GC/MS, *m*/*z* (%) (methyl ester): 310 (13) $[M+2]^+$, 308 (38) $[M]^+$, 139 (100); Anal. Calcd for $C_{15}H_{12}ClFO_3$: C, 61.13; H, 4.10. Found: C, 61.27; H, 4.08.

4.14.5. 2-(4-Chloro-phenoxy)-3-(3-fluoro-phenyl)propanoic acid (14)

50% yield; mp: 125–127 °C; ^{1}H NMR: δ = 3.20–3.32 (m, 2H, CH_2), 4.77–4.81 (m, 1H, CH), 5.97 (bb, 1H, COOH, D_2O exchanged), 6.74–6.79, 6.91–7.08 and 7.18–7.30 (m, 8H, aromatics); ESI-MS *m*/*z* (%) negative: 293 (46) $[M-H]^{-1}$, 165 (100), 127 (38), 121 (19); Anal. Calcd for $C_{15}H_{12}ClFO_3$: C, 61.13; H, 4.10. Found: C, 61.51; H, 4.16.

4.14.6. 2-(4-Chloro-phenoxy)-3-(4-fluoro-phenyl)propanoic acid (15)

57% yield; mp: 108–109 °C; ^{1}H NMR: δ = 3.17–3.30 (m, 2H, CH_2), 4.42 (bb, 1H, COOH, D_2O exchanged), 4.74–4.78 (m, 1H, CH), 6.73–6.78, 6.94–7.12 and 7.19–7.34 (m, 8H, aromatics); GC/MS, *m*/*z* (%) (methyl ester): 310 (12) $[M+2]^+$, 308 (34) $[M]^+$, 181 (57), 139 (100); Anal. Calcd for $C_{15}H_{12}ClFO_3$: C, 61.13; H, 4.10. Found: C, 61.27; H, 4.05.

4.14.7. 2-(4-Chloro-2-fluoro-phenoxy)-3-(3-fluoro-phenyl)propanoic acid (16)

80% yield; mp: 107–108 °C; ^{1}H NMR: δ = 3.23–3.36 (m, 2H, CH_2), 4.79–4.84 (m, 1H, CH), 6.73–6.78, 6.94–7.12 and 7.19–7.34 (m, 8H, 7 aromatics + COOH, D_2O exchanged); GC/MS, *m*/*z* (%) (methyl ester): 328 (11) $[M+2]^+$, 326 (32) $[M]^+$, 181 (36), 139 (100); Anal. Calcd for $C_{15}H_{11}ClF_2O_3$: C, 57.62; H, 3.55. Found: C, 57.76; H, 3.58.

4.14.8. 2-(2-Trifluoromethyl-phenoxy)-3-(3-fluoro-phenyl)propanoic acid (17)

70% yield; mp: 166–168 °C; ^{1}H NMR: δ = 3.28–3.38 (m, 2H, CH_2), 4.96–5.00 (m, 1H, CH), 6.72–7.61 (m, 9H, 8 aromatics + COOH, D_2O exchanged); ESI-MS *m*/*z* (%) negative: 327 (80) $[M-H]^{-1}$, 165 (20), 161 (100), 121 (5); Anal. Calcd for $C_{16}H_{12}F_4O_3$: C, 58.54; H, 3.68. Found: C, 58.83; H, 3.74.

Acknowledgments

This work was accomplished thanks to the financial support of the Università degli Studi di Bari 'Aldo Moro' (Research Fund 2009) and of the CARIPLO Foundation (file 2009-2727).

Supplementary data

Supplementary data associated with this article can be found, in the online version, at doi:10.1016/j.bmc.2012.01.025.

References and notes

1. Berger, J. P.; Akiyama, T. E.; Meinke, P. T. *Trends Pharmacol. Sci.* **2005**, *26*, 244.
2. Kliewer, S. A.; Sundseth, S. S.; Jones, S. A.; Brown, P. J.; Wisely, G. B.; Koble, C. S.; Devchand, P.; Wahli, W.; Willson, T. M.; Lenhard, J. M.; Lehmann, J. M. *Proc. Natl Acad. Sci. USA* **1997**, *94*, 4318.
3. Elisaf, M. *Curr. Med. Res. Opin.* **2002**, *18*, 269.
4. Staels, B.; Dallongeville, J.; Auwerx, J.; Schoonjans, K.; Leitersdorf, E.; Fruchart, J. C. *Circulation* **1998**, *98*, 2088.
5. Evans, R. M.; Barish, G. D.; Wang, Y. X. *Nat. Med.* **2004**, *10*, 355.
6. Semple, R. K.; Chatterjee, V. K.; O'Rahilly, S. *J. Clin. Invest.* **2006**, *116*, 581.
7. Campbell, I. W. *Curr. Mol. Med.* **2005**, *5*, 349.
8. Sprecher, D. L.; Massien, C.; Pearce, G.; Billin, A. N.; Perlstein, I.; Willson, T. M.; Hassall, D. G.; Ancellin, N.; Patterson, S. D.; Lobe, D. C.; Johnson, T. G. *Arterioscler. Thromb. Vasc. Biol.* **2007**, *27*, 359.
9. Reilly, S. M.; Lee, C. H. *FEBS Lett.* **2008**, *582*, 26.
10. Madrazo, J. A.; Kelly, D. P. *J. Mol. Cell. Cardiol.* **2008**, *44*, 968.
11. Schmuth, M.; Jiang, Y. J.; Dubrac, S.; Elias, P. M.; Feingold, K. R. *J. Lipid Res.* **2008**, *49*, 499.
12. Iwashita, A.; Muramatsu, Y.; Yamazaki, T.; Muramoto, M.; Kita, Y.; Yamazaki, S.; Mihara, K.; Moriguchi, A.; Matsuoka, N. *J. Pharmacol. Exp. Ther.* **2007**, *320*, 1087.
13. Peters, J. M.; Hollingshead, H. E.; Gonzalez, F. J. *Clin. Sci. (Lond.)* **2008**, *115*, 107.
14. Willson, T. M.; Brown, P. J.; Sternbach, D. D.; Henke, B. R. *J. Med. Chem.* **2000**, *43*, 527.
15. Henke, B. R. *J. Med. Chem.* **2004**, *47*, 4118.
16. Ebdrup, S.; Pettersson, I.; Rasmussen, H. B.; Deussen, H. J.; Frost Jensen, A.; Mortensen, S. B.; Fleckner, J.; Pridal, L.; Nygaard, L.; Sauerberg, P. *J. Med. Chem.* **2003**, *46*, 1306.
17. Devasthale, P. V.; Chen, S.; Jeon, Y.; Qu, F.; Shao, C.; Wang, W.; Zhang, H.; Cap, M.; Farrelly, D.; Golla, R.; Grover, G.; Harrity, T.; Ma, Z.; Moore, L.; Ren, J.; Seethala, R.; Cheng, L.; Sleph, P.; Sun, W.; Tieman, A.; Wetterau, J. R.; Doweyko,

A.; Chandrasena, G.; Chang, S. Y.; Humphreys, W. G.; Sasseville, V. G.; Biller, S. A.; Ryono, D. E.; Selan, F.; Hariharan, N.; Cheng, P. T. *J. Med. Chem.* **2005**, *48*, 2248.
18. Koyama, H.; Miller, D. J.; Boueres, J. K.; Desai, R. C.; Jones, A. B.; Berger, J. P.; MacNaul, K. L.; Kelly, L. J.; Doebber, T. W.; Wu, M. S.; Zhou, G.; Wang, P. R.; Ippolito, M. C.; Chao, Y. S.; Agrawal, A. K.; Franklin, R.; Heck, J. V.; Wright, S. D.; Moller, D. E.; Sahoo, S. P. *J. Med. Chem.* **2004**, *47*, 3255.
19. Shi, G. Q.; Dropinski, J. F.; McKeever, B. M.; Xu, S.; Becker, J. W.; Berger, J. P.; MacNaul, K. L.; Elbrecht, A.; Zhou, G.; Doebber, T. W.; Wang, P.; Chao, Y. S.; Forrest, M.; Heck, J. V.; Moller, D. E.; Jones, A. B. *J. Med. Chem.* **2005**, *48*, 4457.
20. Grey, A. *Osteoporos. Int.* **2008**, *19*, 129.
21. Shearer, B. G.; Billin, A. N. *Biochim. Biophys. Acta* **2007**, *1771*, 1082.
22. Dropinski, J. F.; Akiyama, T.; Einstein, M.; Habulihaz, B.; Doebber, T.; Berger, J. P.; Meinke, P. T.; Shi, G. Q. *Bioorg. Med. Chem. Lett.* **2005**, *15*, 5035.
23. Reifel-Miller, A.; Otto, K.; Hawkins, E.; Barr, R.; Bensch, W. R.; Bull, C.; Dana, S.; Klausing, K.; Martin, J. A.; Rafaeloff-Phail, R.; Rafizadeh-Montrose, C.; Rhodes, G.; Robey, R.; Rojo, I.; Rungta, D.; Snyder, D.; Wilbur, K.; Zhang, T.; Zink, R.; Warshawsky, A.; Brozinick, J. T. *Mol. Endocrinol.* **2005**, *19*, 1593.
24. Martin, J. A.; Brooks, D. A.; Prieto, L.; Gonzalez, R.; Torrado, A.; Rojo, I.; Lopez de Uralde, B.; Lamas, C.; Ferritto, R.; Dolores Martin-Ortega, M.; Agejas, J.; Parra, F.; Rizzo, J. R.; Rhodes, G. A.; Robey, R. L.; Alt, C. A.; Wendel, S. R.; Zhang, T. Y.; Reifel-Miller, A.; Montrose-Rafizadeh, C.; Brozinick, J. T.; Hawkins, E.; Misener, E. A.; Briere, D. A.; Ardecky, R.; Fraser, J. D.; Warshawsky, A. M. *Bioorg. Med. Chem. Lett.* **2005**, *15*, 51.
25. Burgermeister, E.; Schnoebelen, A.; Flament, A.; Benz, J.; Stihle, M.; Gsell, B.; Rufer, A.; Ruf, A.; Kuhn, B.; Marki, H. P.; Mizrahi, J.; Sebokova, E.; Niesor, E.; Meyer, M. *Mol. Endocrinol.* **2006**, *20*, 809.
26. Allen, T.; Zhang, F.; Moodie, S. A.; Clemens, L. E.; Smith, A.; Gregoire, F.; Bell, A.; Muscat, G. E.; Gustafson, T. A. *Diabetes* **2006**, *55*, 2523.
27. Carmona, M. C.; Louche, K.; Lefebvre, B.; Pilon, A.; Hennuyer, N.; Audinot-Bouchez, V.; Fievet, C.; Torpier, G.; Formstecher, P.; Renard, P.; Lefebvre, P.; Dacquet, C.; Staels, B.; Casteilla, L.; Penicaud, L. *Diabetes* **2007**, *56*, 2797.
28. Kim, M. K.; Chae, Y. N.; Kim, H. S.; Choi, S. H.; Son, M. H.; Kim, S. H.; Kim, J. K.; Moon, H. S.; Park, S. K.; Shin, Y. A.; Kim, J. G.; Lee, C. H.; Lim, J. I.; Shin, C. Y. *Arch. Pharm. Res.* **2009**, *32*, 721.
29. Motani, A.; Wang, Z.; Weiszmann, J.; McGee, L. R.; Lee, G.; Liu, Q.; Staunton, J.; Fang, Z.; Fuentes, H.; Lindstrom, M.; Liu, J.; Biermann, D. H.; Jaen, J.; Walker, N. P.; Learned, R. M.; Chen, J. L.; Li, Y. *J. Mol. Biol.* **2009**, *386*, 1301.
30. Pinelli, A.; Godio, C.; Laghezza, A.; Mitro, N.; Fracchiolla, G.; Tortorella, V.; Lavecchia, A.; Novellino, E.; Fruchart, J. C.; Staels, B.; Crestani, M.; Loiodice, F. *J. Med. Chem.* **2005**, *48*, 5509.
31. Muller, K.; Faeh, C.; Diederich, F. *Science* **2007**, *317*, 1881.
32. Hagmann, W. K. *J. Med. Chem.* **2008**, *51*, 4359.
33. Fracchiolla, G.; Laghezza, A.; Piemontese, L.; Carbonara, G.; Lavecchia, A.; Tortorella, P.; Crestani, M.; Novellino, E.; Loiodice, F. *ChemMedChem* **2007**, *2*, 641.
34. Gregoire, F. M.; Zhang, F.; Clarke, H. J.; Gustafson, T. A.; Sears, D. D.; Favelyukis, S.; Lenhard, J.; Rentzeperis, D.; Clemens, L. E.; Mu, Y.; Lavan, B. E. *Mol. Endocrinol.* **2009**, *23*, 975.
35. Montanari, R.; Saccoccia, F.; Scotti, E.; Crestani, M.; Godio, C.; Gilardi, F.; Loiodice, F.; Fracchiolla, G.; Laghezza, A.; Tortorella, P.; Lavecchia, A.; Novellino, E.; Mazza, F.; Aschi, M.; Pochetti, G. *J. Med. Chem.* **2008**, *51*, 7768.
36. Carbonara, G.; Fracchiolla, G.; Loiodice, F.; Tortorella, P.; Conte-Camerino, D.; De Luca, A.; Liantonio, A. *Il Farmaco.* **2001**, *56*, 749.
37. Wang, W.; Devasthale, P.; Farrelly, D.; Gu, L.; Harrity, T.; Cap, M.; Chu, C.; Kunselman, L.; Morgan, N.; Ponticiello, R.; Zebo, R.; Zhang, L.; Locke, K.; Lippy, J.; O'Malley, K.; Hosagrahara, V.; Kadiyala, P.; Chang, C.; Muckelbauer, J.; Doweyko, A. M.; Zahler, R.; Ryono, D.; Hariharan, N.; Cheng, P. T. *Bioorg. Med. Chem. Lett.* **2008**, *18*, 1939.
38. Glide, version 5.7; Schrodinger, LLC: New York, 2011.
39. (a) Dunitz, J. D.; Taylor, R. *Chem. Eur. J.* **1997**, *3*, 89; (b) Dunitz, J. D. *ChemBioChem* **2004**, *5*, 614.
40. Pochetti, G.; Godio, C.; Mitro, N.; Caruso, D.; Galmozzi, A.; Scurati, S.; Loiodice, F.; Fracchiolla, G.; Tortorella, P.; Laghezza, A.; Lavecchia, A.; Novellino, E.; Mazza, F.; Crestani, M. *J. Biol. Chem.* **2007**, *282*, 17314.
41. Leslie, A.; Janisch, S. *Health Serv. J.* **1992**, *102*, 26.
42. Brunger, A. T.; Adams, P. D.; Clore, G. M.; DeLano, W. L.; Gros, P.; Grosse-Kunstleve, R. W.; Jiang, J. S.; Kuszewski, J.; Nilges, M.; Pannu, N. S.; Read, R. J.; Rice, L. M.; Simonson, T.; Warren, G. L. *Acta Crystallogr., Sect. D* **1998**, *54*, 905.
43. Nolte, R. T.; Wisely, G. B.; Westin, S.; Cobb, J. E.; Lambert, M. H.; Kurokawa, R.; Rosenfeld, M. G.; Willson, T. M.; Glass, C. K.; Milburn, M. V. *Nature* **1998**, *395*, 137.
44. Maestro, version 9.2; Schrödinger, LLC, New York, NY, 2011.
45. DeLano, Warren L. The PyMOL Molecular Graphics System. DeLano Scientific LLC, San Carlos, CA, USA. http://www.pymol.org/.
46. LigPrep, version 2.5; Schrödinger, LLC, New York, NY, 2011.
47. Epik, version 2.2; Schrödinger, LLC: New York, 2009.
48. Friesner, R. A.; Banks, J. L.; Murphy, R. B.; Halgren, T. A.; Klicic, J. J.; Mainz, D. T.; Repasky, M. P.; Knoll, E. H.; Shelley, M.; Perry, J. K.; Shaw, D. E.; Francis, P.; Shenkin, P. S. *J. Med. Chem.* **2004**, *47*, 1739.
49. Raspe, E.; Madsen, L.; Lefebvre, A.-M.; Leitersdorf, I.; Gelman, L.; Peinado-Onsurbe, J.; Dallongeville, J.; Fruchart, J.-C.; Berge, R.; Staels, B. *J. Lipid. Res.* **1999**, *40*, 2099.
50. Hollons, T.; Yoshimura, F. K. *Anal. Biochem.* **1989**, *182*, 411.